< Electronic Supplementary Information >

Straightforward formation of dianionic acetonylate: self-assembly of mercury(II) with pyridyl donor ligands in acetone

Kangsan Hong,[a] Sangwoo Lim,[a] Heehun Moon,[a] Dongwon Kim,[a] Dongwook Kim[b] and Ok-Sang Jung*,[a]

[a] Department of Chemistry, Pusan National University, Busan 46241, Republic of Korea

[b] Center for Hydrocarbon Functionalizations, IBS, Daejon 34141, Republic of Korea

Fax: (+82) 51-5163522; Tel: (+82) 51-5103240; E-mail: oksjung@pusan.ac.kr

Experimental Procedures

Materials and Measurements.
All of the chemicals including mercury(II) perchlorate, 3-bromopyridine, and *n*-butyllithium (Aldrich) and 1,3-bis(chlorodimethylsilyl)propane (Gelest) were used without further purification. Naphthalene-2,6-diyl diisonicotinate (L*) was synthesized according to the literature.[1] ^{1}H NMR spectra were recorded on a Varian Mercury Plus 400 MHz (chemical shifts are relative to tetramethylsilane [TMS] as internal standard in δ values [ppm]). ^{13}C NMR spectra were recorded on a AVANCE NEO 500. ^{1}H-^{13}C 2D-HMBC NMR, and ^{1}H-^{13}C 2D-HMQC NMR spectra were recorded on an Agilent NMR System 600. Infrared spectra were obtained on a Nicolet 380 FT-IR spectrophotometer with samples prepared as KBr pellets. Thermal analyses were carried out under N_2 at a scan rate of 10°C/min using a Labsys TGA-DSC 1600.

Synthesis of 1,3-Bis(dimethyl(pyridin-3-yl)silyl)propane (L).
To a solution of 3-bromopyridine (6.32 g, 40 mmol) in dry diethyl ether (100 mL) under a nitrogen gas atmosphere, *n*-butyllithium (16 mL of 2.5 M solution in *n*-hexane, 40 mmol) was added dropwise at −78°C. The resultant mixture was stirred for 90 min at 0°C. Then, 1,3-bis(chlorodimethylsilyl)propane (4.59 g, 20 mmol) in dry diethyl ether (50 mL) was slowly added to the above brown suspension at −78°C, and then the reaction mixture was stirred for 12 h at room temperature. Distilled water (200 mL) was added, and then the organic layer was separated. The crude product was purified by column chromatography using a mixture of ethyl acetate and *n*-hexane as an eluent. The solvent was evaporated to obtain a yellowish brown viscous liquid in a 76% yield (4.78 g). Anal. Calcd for $C_{17}H_{26}N_2Si_2$: C, 64.91; H, 8.34; N, 8.91%. Found: C, 64.20; H, 8.36; N, 8.77%. IR (KBr pellet, cm^{-1}): 3028 (m), 2963 (m), 2913 (m), 1571 (m), 1473 (w), 1392 (s), 1330 (w), 1253 (s), 1122 (s), 1027 (m), 907 (s), 809 (s), 798 (s), 770 (s), 490 (m). ^{1}H NMR (Me_2SO-d_6, 400 MHz, ppm): 8.60 (s, 2H), 8.54 (d, J = 4.63 Hz, 2H), 7.82 (m, J = 11.26 Hz, 2H), 7.34 (d, J = 13.38 Hz, 2H), 1.33 (m, J = 32.39 Hz, 2H), 0.80 (m, J = 16.26 Hz, 4H), 0.23 (s, 12H).

$[Hg_4(ClO_4)_4(CH_2COCH_2)_2L_2]\cdot CH_3COCH_3$.
An acetone solution (2.0 mL) of $Hg(ClO_4)_2$ (7.99 mg, 0.02 mmol) was carefully layered onto a diethyl ether solution of L (12.56 mg, 0.02 mmol). After 1 weeks, white crystals suitable for X-ray single crystallography were obtained in a 70% yield. Anal. Calcd for $C_{43}H_{66}Cl_4Hg_4N_4O_{19}Si_4$: C, 25.83 H, 3.32; N, 2.80%. Found: C,25.70; H,3.34; N,2.82%. IR (KBr pellet, cm^{-1}): 3485(b), 2914(m), 1719(m), 1615(m), 1593(w), 1404(m), 1250(m), 1090(s), 906(m), 826(m), 700(m), 625(w), 528(w), 470(w). ^{1}H NMR (Me_2SO-d_6, 400 MHz, ppm): 8.77 (m, J = 17.39 Hz, 4H), 8.35 (d, J = 7.25 Hz, 2H), 7.85 (d, J = 13.13 Hz, 2H), 2.77 (s, 2H), 2.73 (s, 2H), 2.18 (s, 3H), 1.32 (m, J = 30.26 Hz, 2H), 0.84 (m, J = 28.85 Hz 4H), 0.30 (s, 12H).

$[Hg_4(ClO_4)_4(CD_2COCD_2)_2L_2]\cdot CD_3COCD_3$.
An acetone-d_6 solution (2.0 mL) of $Hg(ClO_4)_2$ (7.99 mg, 0.02 mmol) was carefully layered

onto a diethyl ether solution of L (12.56 mg, 0.02 mmol). After 1 weeks, white crystals suitable for X-ray single crystallography were obtained in a 67% yield. Anal. Calcd for $C_{43}H_{58}D_8Cl_4Hg_4N_4O_{19}Si_4$: C, 25.83 H, 3.71; N, 2.79%. Found: C,25.70; H,3.64; N,2.82%. IR (KBr pellet, cm^{-1}): 3264(b), 2916(b), 1710(m), 1617(m), 1593(m), 1402(m), 1252(m), 1090(s), 906(m), 826(m), 702(w), 628(m), 460(w). ^{1}H NMR (Me_2SO-d_6, 400 MHz, ppm): 8.74 (m, J = 5.50 Hz, 4H), 8.24 (d, J = 8.38 Hz, 2H), 7.77 (d, J = 10.76 Hz, 2H), 1.32 (m, J = 27.89 Hz, 2H), 0.84 (m, J = 24.76 Hz, 4H), 0.28 (s, 12H).

$[Hg_2(ClO_4)_2(CH_2COCH_3)_2L^*]\cdot CH_3COCH_3$.

An acetone solution (2 mL) of $Hg(ClO_4)_2$ (3.99 mg, 0.01 mmol) was slowly diffused into a dichloromethane solution (2 mL) of L^* (3.70 mg, 0.01 mmol). Colorless crystals of $[Hg_2(ClO_4)_2(CH_2COCH_3)_2L^*]\cdot CH_3COCH_3$ formed at the interface and were obtained in 3 days in a 74% yield. Anal. Calcd for $C_{31}H_{30}Cl_2Hg_2N_2O_{15}$: C, 32.60; H, 2.64; N, 2.45%. Found: C, 32.07; H, 2.45; N, 2.59%. IR (KBr, cm^{-1}): 1737(s, C=O), 1666(m), 1429(m), 1361(m), 1278(s), 1209(s), 1143(s), 1083(s), 1058(s), 1058(s), 622(s). ^{1}H NMR (Me_2SO-d_6, ppm): 9.03 (d, J = 6.26 Hz, 4H), 8.31(d, J = 6.26 Hz, 4H), 8.13(d, J = 8.61 Hz, 2H), 8.02 (s, 2H), 7.65 (d, J = 8.61 Hz, 2H), 2.73(s, 2H), 2.17(s, 3H).

Crystal Structure Determination.

All X-ray data of $[Hg_4(ClO_4)_2(CH_2COCH_2)L_2]\cdot CH_3COCH_3$, $[Hg_4(ClO_4)_2(CD_2COCD_2)L_2]\cdot CD_3COCD_3$, and $[Hg_2(ClO_4)_2(CH_2COCH_3)_2L^*]\cdot CH_3COCH_3$ were collected on a Bruker SMART automatic diffractometer with graphite-monochromated Mo Kα radiation (λ = 0.71073 Å). Thirty-six (36) frames of 2D diffraction images were collected and processed to obtain the cell parameters and orientation matrix. The data were corrected for Lorentz and polarization effects. The absorption effects were corrected using the multi-scan method (SADABS).[2] The structures were solved using the direct method (SHELXS) and refined by full-matrix least squares techniques (SHELXL 2018/3).[3] The non-hydrogen atoms were refined anisotropically, and the hydrogen atoms were placed in calculated positions and refined only for the isotropic thermal factors. The crystal parameters and procedural information corresponding to the data collection and structure refinement are listed in Tables S1 and S2. The volumes of solvate molecules in $[Hg_4(ClO_4)_4(CH_2COCH_2)_2L_2]\cdot CH_3COCH_3$, $[Hg_4(ClO_4)_4(CD_2COCD_2)_2L_2]\cdot CD_3COCD_3$, and $[Hg_2(ClO_4)_2(CH_2COCH_3)_2L^*]\cdot CH_3COCH_3$ were 8.8% (269.6 Å^3/ 3055.8 Å^3), 7.0% (215.5 Å^3/ 3061.8 Å^3) and 13.4%(120.7 Å^3/ 899.8 Å^3) respectively, on the basis of PLATON/SOLV calculation,[4] and their all solvate molecules were squeezed.

References

1 L. Yang, D. Kim, S. Hyun, Y.-A. Lee and O.-S. Jung, *Transit. Met. Chem.*, 2020, **45**, 139-145.
2 G. M. Sheldrick, *Program for empirical absorption correction of area detector data*, SADABS, 1996.
3 G. M. Sheldrick, *Acta Crystallographica Section C: Structural Chemistry*, 2015, **71**, 3-8.
4 A. L. Spek, *PLATON: A Multipurpose Crystallographic Tool; Utrecht University: Utrecht, The Netherlands*, 2003.

Table S1 Crystal data and structural refinements for $[Hg_4(ClO_4)_4(CH_2COCH_2)_2L_2]\cdot CH_3COCH_3$, $[Hg_4(ClO_4)_4(CD_2COCD_2)_2L_2]\cdot CD_3COCD_3$, and $[Hg_2(ClO_4)_2(CH_2COCH_3)_2L^*]\cdot CH_3COCH_3$

	$[Hg_4(ClO_4)_4(CH_2COCH_2)_2L_2]$ $\cdot CH_3COCH_3$	$[Hg_4(ClO_4)_4(CD_2COCD_2)_2L_2]$ $\cdot CD_3COCD_3$	$[Hg_2(ClO_4)_2(CH_2COCH_3)_2L^*]$ $\cdot CH_3COCH_3$
Formula	$C_{40}H_{60}Cl_4Hg_4N_4O_{18}Si_4$	$C_{40}H_{60}Cl_4Hg_4N_4O_{18}Si_4$	$C_{14}H_{12}ClHgNO_7$
M_w	1941.44	1941.44	542.29
Cryst. sys.	Monoclinic	Monoclinic	Triclinic
Space group	$C2/m$	$C2/m$	$P\bar{1}$
a (Å)	21.1453(8)	21.124(1)	7.7679(9)
b (Å)	17.4789(7)	17.421(1)	9.396(1)
c (Å)	8.6030(3)	8.6306(5)	13.225(2)
α (°)	-	-	89.233(1)
β (°)	104.821(1)	105.284(2)	84.705(1)
γ (°)	-	-	69.453(1)
V (Å^3)	3073.8(2)	3063.6(3)	899.8(2)
Z	2	2	2
ρ (g cm^{-3})	2.098	2.105	2.001
μ (mm^{-1})	10.275	10.309	8.734
R_{int}	0.0589	0.0638	0.0496
GoF on F^2	1.212	1.173	1.053
R_1 [$I>2\sigma(I)$][a]	0.0612	0.0887	0.0395
wR_2 (all data)[b]	0.1652	0.2459	0.1050

[a] $R_1 = \Sigma||F_o| - |F_c||/\Sigma|F_o|$, [b] $wR_2 = (\Sigma[w(F_o^2 - F_c^2)^2]/\Sigma[w(F_o^2)^2])^{1/2}$

Table S2 Selected bond lengths (Å) and angles (°) for $[Hg_4(ClO_4)_4(CH_2COCH_2)_2L_2]\cdot CH_3COCH_3$, $[Hg_4(ClO_4)_4(CD_2COCD_2)_2L_2]\cdot CD_3COCD_3$, and $[Hg_2(ClO_4)_2(CH_2COCH_3)_2L^*]\cdot CH_3COCH_3$

$[Hg_4(ClO_4)_4(CH_2COCH_2)_2L_2]\cdot CH_3COCH_3$		$[Hg_4(ClO_4)_4(CD_2COCD_2)_2L_2]\cdot CD_3COCD_3$		$[Hg_2(ClO_4)_2(CH_2COCH_3)_2L^*]\cdot CH_3COCH_3$	
Hg(1)-N(2B)	2.06(1)	Hg(1)-N(2B)	2.08(2)	Hg(1)-C(1)	2.079(7)
Hg(1)-C(11A)	2.10(1)	Hg(1)-C(11A)	2.131(1)	Hg(1)-N(12L)	2.135(5)
Hg(1)-N(2A)	2.22(2)	Hg(1)-N(2)	2.25(3)		
Hg(1)-O(5A)	2.47(2)	Hg(1)-O(5A)	2.44(3)		
Hg(1)-O(13)$^{\#1}$	2.662(7)	Hg(1)-O(13)$^{\#1}$	2.63(1)		
N(2B)-Hg(1)-C(11A)	174.2(6)	N(2B)-Hg(1)-C(11A)	172.9(9)	C(1)-Hg(1)-N(12L)	175.2(2)
C(11A)-Hg(1)-N(2A)	173.2(6)	C(11A)-Hg(1)-N(2)	176(1)	C(11L)-N(12L)-Hg(1)	120.8(4)
N(2B)-Hg(1)-O(5A)	74.8(8)	N(2B)-Hg(1)-O(5A)	19(1)	C(13L)-N(12L)-Hg(1)	119.5(5)
C(11A)-Hg(1)-O(5A)	105.3(6)	C(11A)-Hg(1)-O(5A)	104.5(9)	C(1E)-C(2E)-Hg(1)	109.5(5)
N(2A)-Hg(1)-O(5A)	81.5(8)	N(2A)-Hg(1)-O(5A)	79(1)		
C(3A)-N(2A)-Hg(1)	128(1)	N(2B)-Hg(1)-O(13)$^{\#1}$	88.4(8)		
C(7A)-N(2A)-Hg(1)	112(1)	C(11A)-Hg(1)-O(13)$^{\#1}$	97.0(6)		
C(3B)-N(2B)-Hg(1)	122.1(9)	N(2B)-Hg(1)-O(13)$^{\#1}$	88.4(8)		
C(7B)-N(2B)-Hg(1)	118(1)	O(5A)-Hg(1)-O(13)$^{\#1}$	98.3(9)		
O(2A)#1-O(5A)-Hg(1)	156(7)	C(11A)-Hg(1)-Hg(1)$^{\#2}$	77.4(5)		
Cl(1A)-O(5A)-Hg(1)	133(1)	N(2A)-Hg(1)-Hg(1)$^{\#2}$	98.4(1)		
Cl(1A)#1-O(5A)-Hg(1)	127(1)	O(5A)-Hg(1)-Hg(1)$^{\#2}$	145.9(9)		
C(12A)-C(11A)-Hg(1)	109.7	O(13)#1-Hg(1)-Hg(1)$^{\#2}$	48.2(2)		
		C(3A)-N(2A)-Hg(1)	135(2)		
		C(7A)-N(2A)-Hg(1)	105(2)		

$^{\#1}$-x+1,-y+1,-z+2
$^{\#2}$ x,-y+1,z
$^{\#3}$-x+1,y,-z+2

$^{\#1}$-x+1,-y+1,-z+2
$^{\#2}$ -x+1,y,-z+2
$^{\#3}$ x,-y+1,z

$^{\#1}$ -x+2,-y+1,-z+2

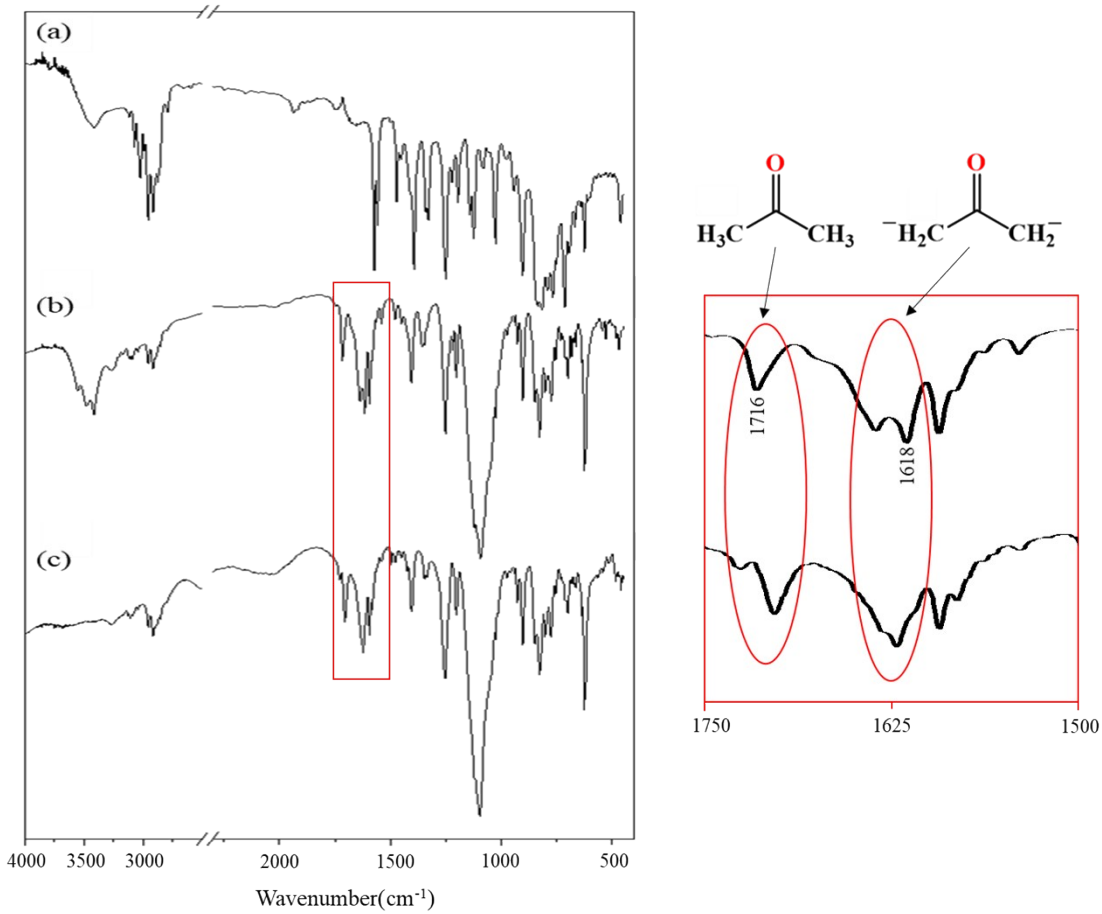

Fig. S1 IR spectra for L (a), $[Hg_4(ClO_4)_4(CH_2COCH_2)_2L_2]\cdot CH_3COCH_3$ (b), and $[Hg_4(ClO_4)_4(CD_2COCD_2)_2L_2]\cdot CD_3COCD_3$ (c).

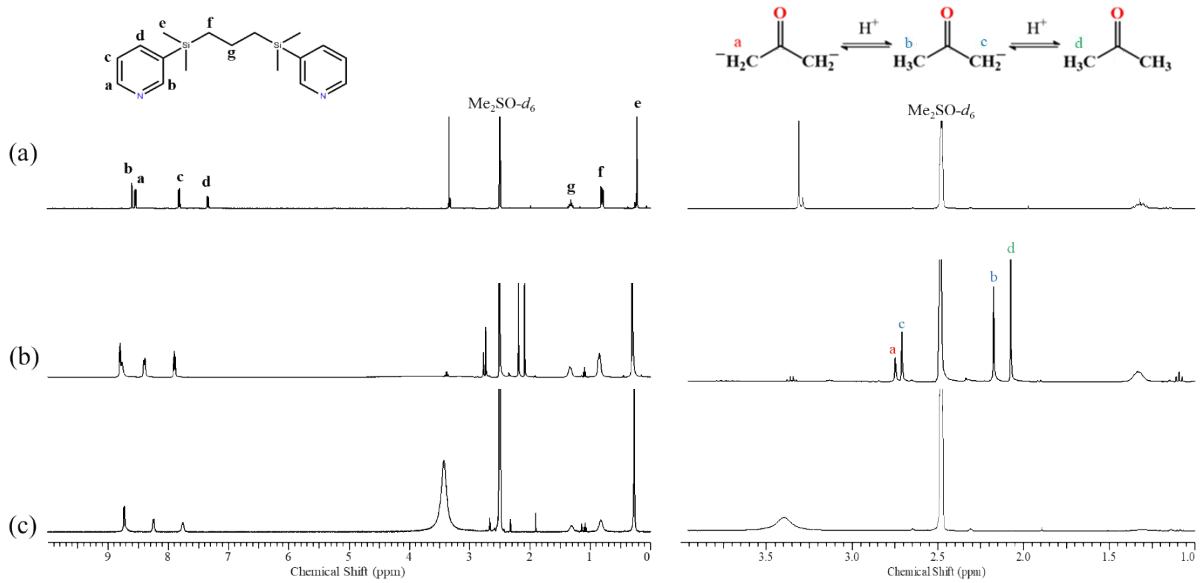

Fig. S2 ^{1}H NMR spectra for L (a), $[Hg_4(ClO_4)_4(CH_2COCH_2)_2L_2]\cdot CH_3COCH_3$ (b), and $[Hg_4(ClO_4)_4(CD_2COCD_2)_2L_2]\cdot CD_3COCD_3$ (c) in Me_2SO-d_6.

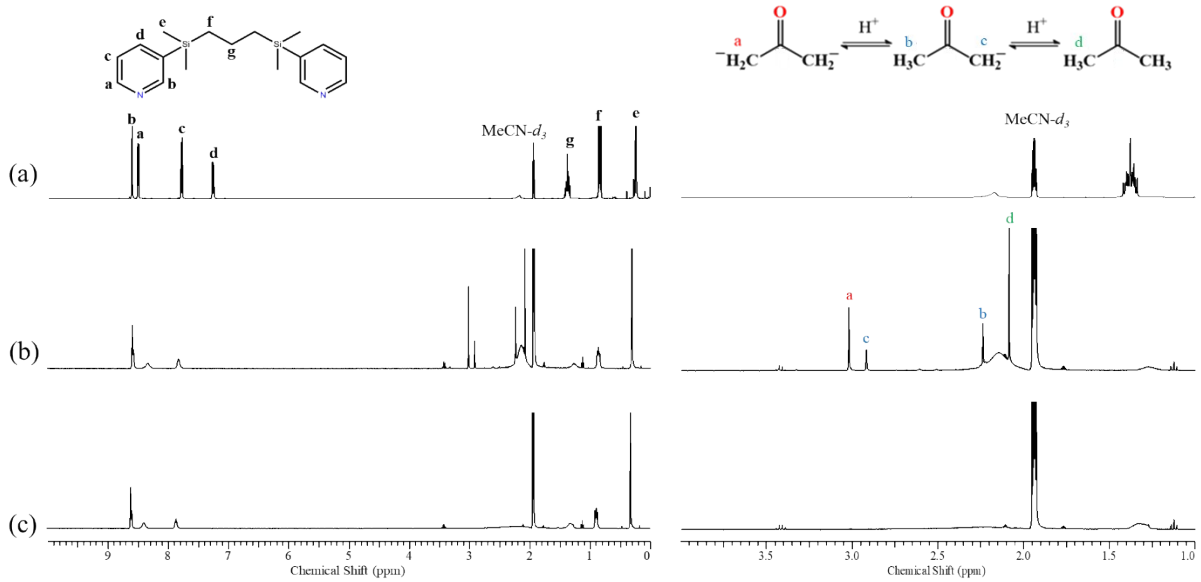

Fig. S3 ^{1}H NMR spectra for L (a), $[Hg_4(ClO_4)_4(CH_2COCH_2)_2L_2]\cdot CH_3COCH_3$ (b), and $[Hg_4(ClO_4)_4(CD_2COCD_2)_2L_2]\cdot CD_3COCD_3$ (c) in MeCN-d_3.

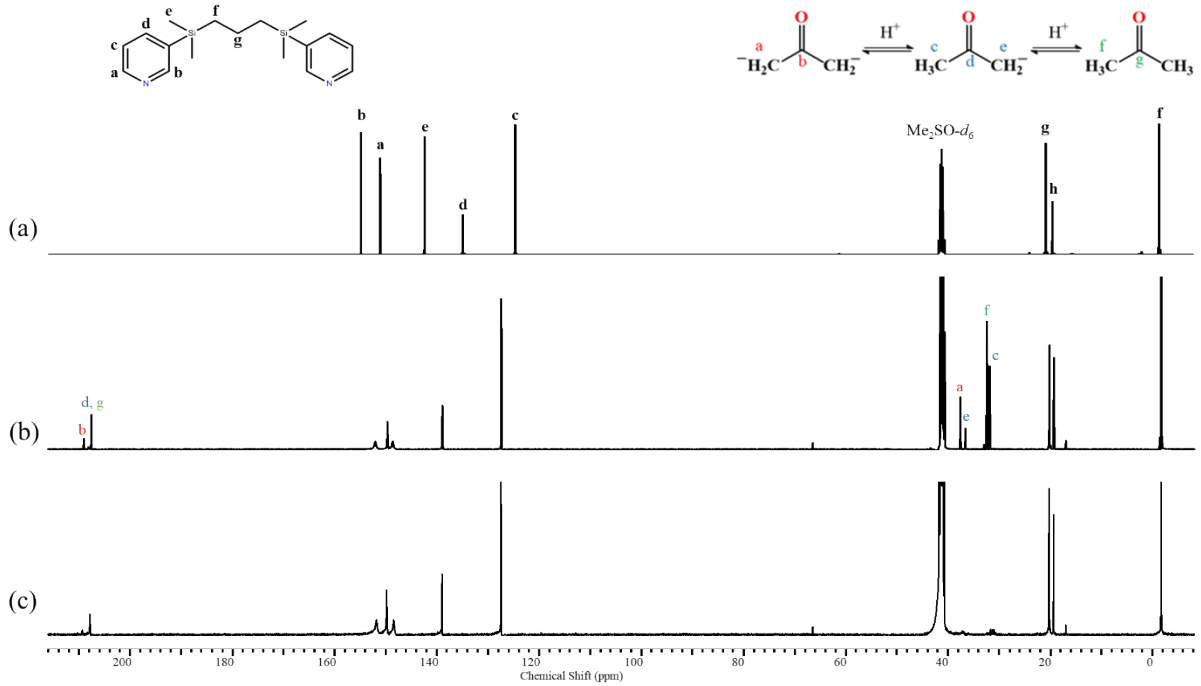

Fig. S4 ^{13}C NMR spectra for L (a), $[Hg_4(ClO_4)_4(CH_2COCH_2)_2L_2]\cdot CH_3COCH_3$ (b), and $[Hg_4(ClO_4)_4(CD_2COCD_2)_2L_2]\cdot CD_3COCD_3$ (c) in Me_2SO-d_6.

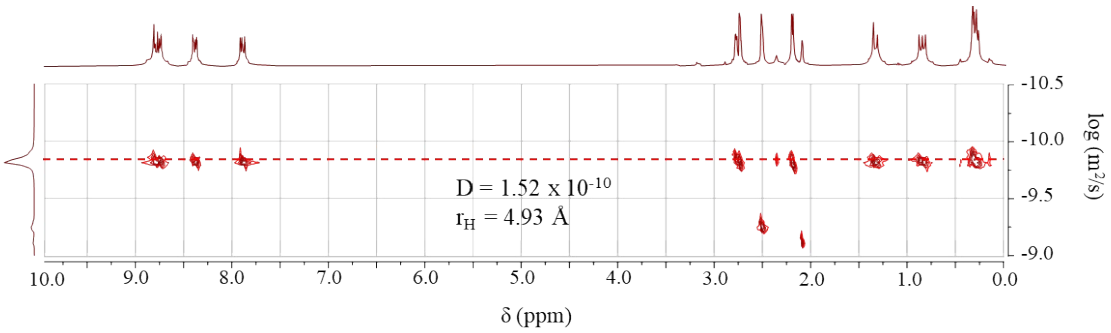

Fig. S5 ^{1}H 2D-DOSY NMR spectrum of $[Hg_4(ClO_4)_4(CH_2COCH_2)_2L_2]\cdot CH_3COCH_3$ in Me_2SO-d_6.

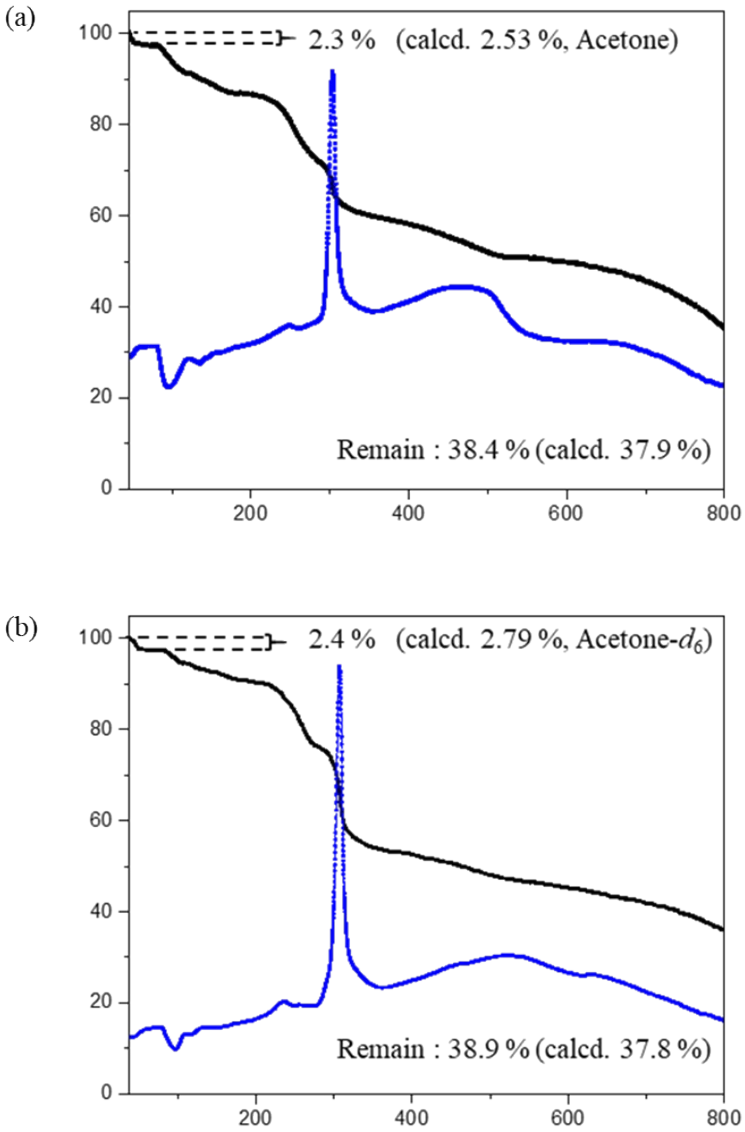

Fig. S6 TGA and DSC curves for $[Hg_4(ClO_4)_4(CH_2COCH_2)_2L_2]\cdot CH_3COCH_3$ (a) and $[Hg_4(ClO_4)_4(CD_2COCD_2)_2L_2]\cdot CD_3COCD_3$ (b).

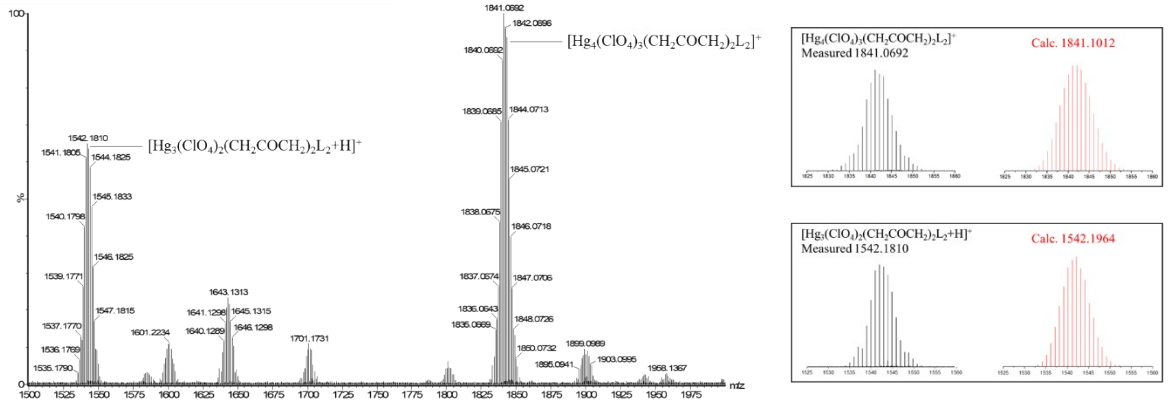

Fig. S7 ESI-Mass data of $[Hg_4(ClO_4)_4(CH_2COCH_2)_2L_2]\cdot CH_3COCH_3$.

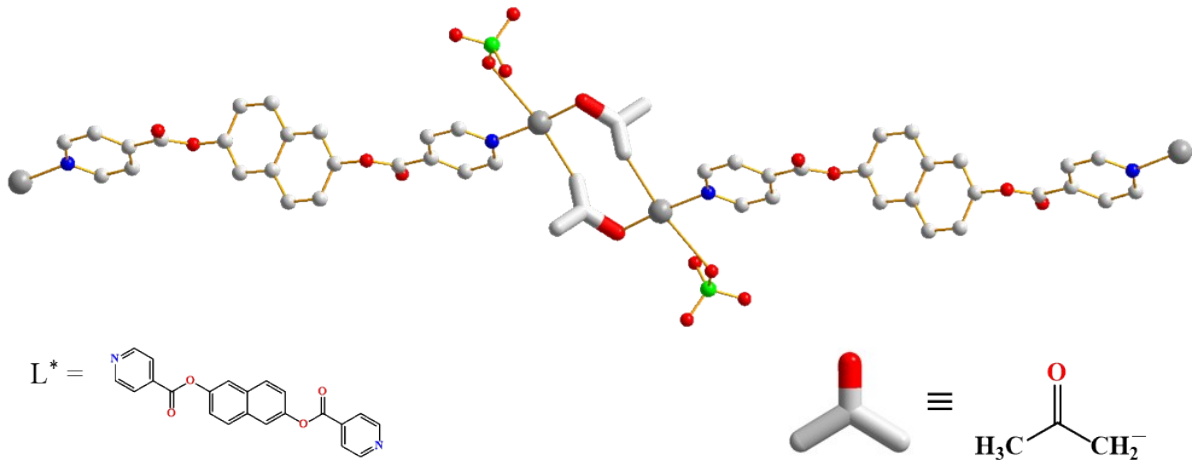

Fig. S8 Crystal structure of $[Hg_2(ClO_4)_2(CH_2COCH_3)_2L^*]\cdot CH_3COCH_3$ including the monoanionic acetonylate.

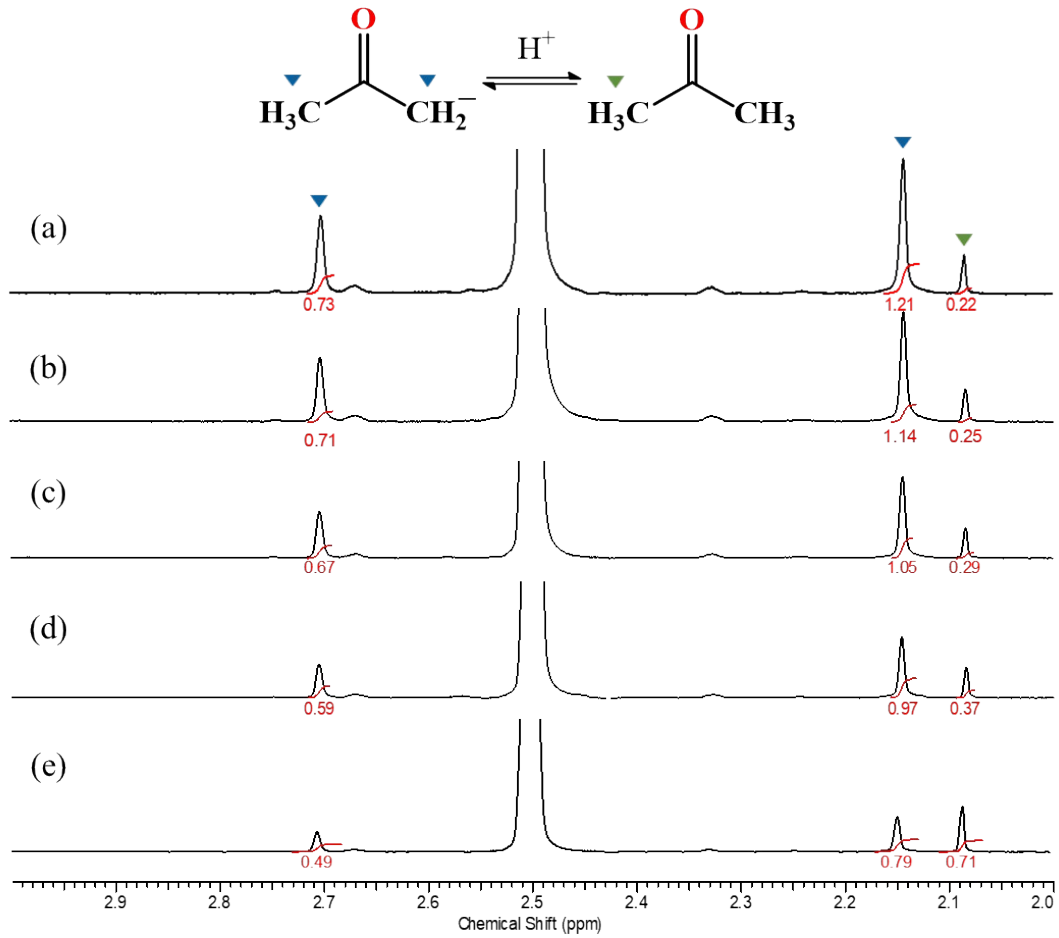

Fig. S9 ^{1}H NMR of $[Hg_2(ClO_4)_2(CH_2COCH_3)_2L^*]\cdot CH_3COCH_3$ (a), $[Hg_2(ClO_4)_2(CH_2COCH_3)_2L^*]\cdot CH_3COCH_3$ + H_2O 1µL (b), $[Hg_2(ClO_4)_2(CH_2COCH_3)_2L^*]\cdot CH_3COCH_3$ + H_2O 1µL after 1 h at RT (c), $[Hg_2(ClO_4)_2(CH_2COCH_3)_2L^*]\cdot CH_3COCH_3$ + H_2O 1µL after 6 h at RT (d), and $[Hg_2(ClO_4)_2(CH_2COCH_3)_2L^*]$ + H_2O 1µL after 24 h at RT (e) showing the equilibrium between $CH_3COCH_2^-$ and CH_3COCH_3.

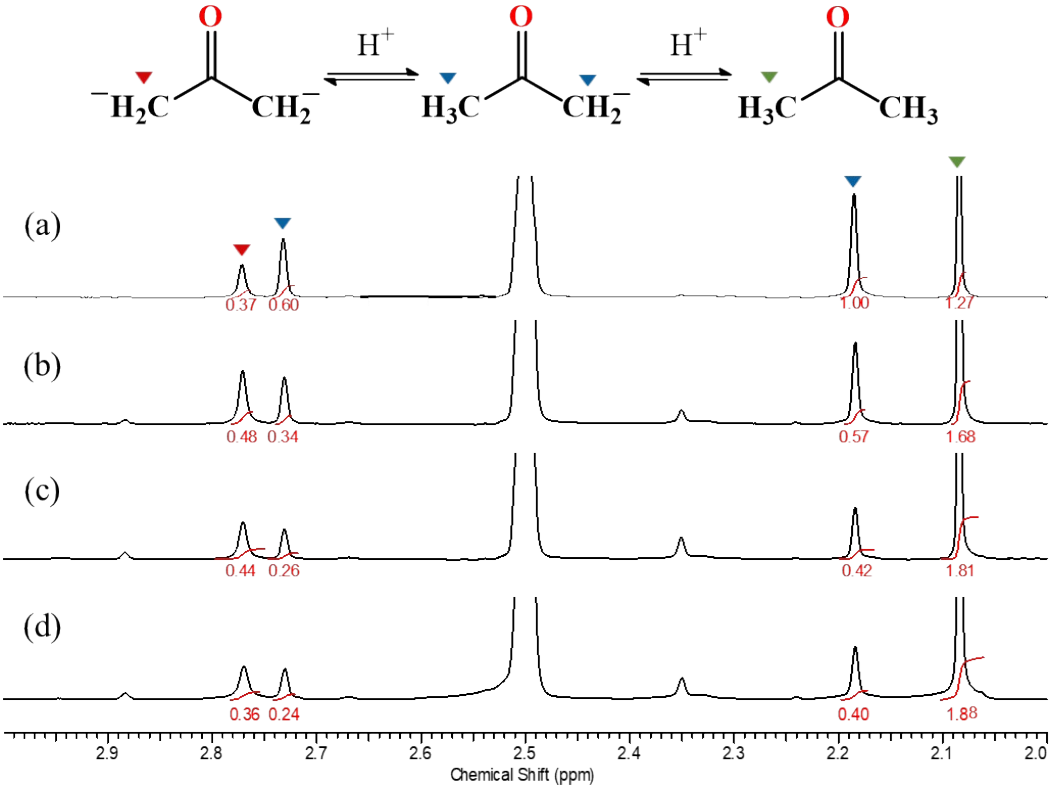

Fig. S10 ^{1}H NMR of $[Hg_4(ClO_4)_4(CH_2COCH_2)_2L_2]\cdot CH_3COCH_3$ (a), $[Hg_4(ClO_4)_4(CH_2COCH_2)_2L_2]\cdot CH_3COCH_3$ after 1 h at 100ºC (b), $[Hg_4(ClO_4)_4(CH_2COCH_2)_2L_2]\cdot CH_3COCH_3$ after 6 h at 100ºC (c), and $[Hg_4(ClO_4)_4(CH_2COCH_2)_2L_2]\cdot CH_3COCH_3$ after 24 h at 100ºC (d) showing the equilibrium between $^{-}CH_2COCH_2^{-}$, $CH_3COCH_2^{-}$ and CH_3COCH_3.